

## Improvement the Corrosion Resistance of pure Al, Al-Si and Al-Zn alloys by Nanoalumina Coating

Asst. Prof. Dr. Rana Afif Majed

University of Technology – Materials Engineering Department

Iraq – Baghdad

### Abstract

This work involves applying the coating by nanoalumina using atomization technique to improve corrosion resistance of pure Al, Al-Si and Al-Zn alloys. Potentiodynamic polarization method was carried out for uncoated and coated specimens in 3.5% NaCl solution at room temperature. Corrosion parameters were measured to know the protection efficiency obtained for nanocoatings. The data of corrosion indicate that nanoalumina coatings corrosion potentials shift toward active direction and corrosion current densities toward lower values. Good protection efficiency was obtained especially for coated pure Al equal to 80%.

Cyclic polarization curves were achieved to know the susceptibility to pitting corrosion, nanocoatings lead to shift forward and reverse scan toward active direction and lower hysteresis loops.

**Key word:** Nanocoatings; Aluminium; Atomization.

### Introduction

Pitting corrosion occurs on more or less passivated metals and alloys in environments containing chloride, bromide, iodide or perchlorate ions when the electrode potential exceeds a critical value, the pitting potential, which depends on various conditions. Aluminium is liable to pitting corrosion in media containing chloride. Among aluminium alloys, those alloyed with magnesium and/or manganese and the commercially pure grades are the best ones. These perform quite well in seawater. Aluminium with magnesium (e.g. AlMg 4.5 Mn) is used in hulls of high-speed vessels and small boats, in deck structures on ships and boats and in helicopter decks on oil and gas platforms. AlMgSi alloys will normally acquire somewhat larger pits, but they are used in profiles, e.g. in marine atmospheres.

There are many methods were applied to protect metals and alloys against corrosion, the most important methods are coatings with more or less noble metals. Nanotechnology gives new field to applied nanocoatings to protect many metallic surfaces.

Jaephil et al. in 2000 studied a high-performance LiCoO<sub>2</sub> cathode fabricated by a sol-gel coating of Al<sub>2</sub>O<sub>3</sub> to the LiCoO<sub>2</sub> particle surfaces and subsequent heat treatment at 600°C for 3 h. Unlike bare LiCoO<sub>2</sub>, the Al<sub>2</sub>O<sub>3</sub>-coated LiCoO<sub>2</sub> cathode exhibits no decrease in its original specific capacity of 174 mA h/g (vs lithium metal) and excellent capacity retention (97% of its initial capacity) between 4.4 and 2.75 V after 50 cycles.

Similar excellent capacity retention of the coated  $\text{LiCoO}_2$  is also observed in a Li ion cell (C/LiCoO<sub>2</sub>) [1].

You et al. in 2000 used the plasma spray technique to deposit coatings with reconstituted nanostructured  $\text{Al}_2\text{O}_3/\text{TiO}_2$  powders. The abrasive wear resistance of the ceramic coatings was evaluated using diamond abrasives. The result showed that the abrasive wear resistance of the coatings produced using the nanostructured  $\text{Al}_2\text{O}_3/\text{TiO}_2$  powders is greatly improved compared with the coating produced using the conventional  $\text{Al}_2\text{O}_3/\text{TiO}_2$  powder. The highest abrasion resistance of the coating sprayed with nanostructured  $\text{Al}_2\text{O}_3/\text{TiO}_2$  powder is about four times that of the coating sprayed with the conventional  $\text{Al}_2\text{O}_3/\text{TiO}_2$  powder [2]. Also, Jordan et al. in 2001 used plasma spraying of reconstituted nanostructured powders using various processing conditions to produce nanostructured alumina–titania coatings. Properties of the nanostructured coatings were related to processing conditions through a critical plasma spray parameter that in turn, can be related to the amount of unmelted powder incorporated into the final coating [3].

While Jinda et al. in 2003 studied coating gold nanoparticle surfaces with peptide molecules which expand the application potentialities of these nanomaterials in biomedical sciences. This work demonstrates that the chiral integrity of each amino acid is maintained and the high coupling efficiency could be achieved in the peptide elongation route for coating gold nanoparticles [4].

Sheng et al. in 2003 studied ultra-fine  $\text{Al}_2\text{O}_3$ ,  $\text{ZrO}_2$  and SiC powders to co-deposition with Ni by electroplating from a nickel sulfamate bath. An electroplating additive  $\text{Na}_3\text{Co}(\text{NO}_2)_6$  can promote the co-deposition of the SiC particles, but the  $\text{Al}_2\text{O}_3$  and  $\text{ZrO}_2$  particles can form composite layers without the assistance of the additive [5].

Brian et al. in 2004 studied development of the operational basis for rapid and controlled deposition of crystal coatings from particles of a wide size range. They deposited structured coatings by dragging with constant velocity a small volume of liquid confined in a meniscus between two plates. Two types of structured coatings were characterized: latex colloidal crystals and thin layers from metallic nanoparticles [6].

Yulu et al. in 2004 studied coating or encapsulation of nanoparticles due to the small size, high surface energy, and high surface area of the nanoparticles. In this paper they describe a new method using supercritical  $\text{CO}_2$  as an anti-solvent (SAS) for nanoparticle coating/encapsulation. A model system, using silica nanoparticles as host particles and Eudragit polymer as the coating material, was chosen for this purpose [7].

Xinhua et al. in 2004 studied nanostructured and conventional alumina–3 wt.% titania coatings to deposit by air plasma spraying (APS). The microstructure and phase composition of the coatings were characterized by X-ray diffraction (XRD), scanning electron microscopy (SEM) and transmission electron microscopy (TEM). Mechanical properties including hardness, adhesion strength, crack extension force ( $G_C$ ) and sliding wear rate were measured [8].

Sheng et al. in 2004 studied nano-alumina particles (80 nm) which easily agglomerated into larger particles in a nickel sulfamate bath with an average diameter of about 1109 nm. This leads to low alumina content in the composite coating. In this study, the diameter of alumina agglomerates was reduced with the decrease in electrolyte concentration [9]. Hong et al. in 2005 studied a wet chemical method to prepare Al<sub>2</sub>O<sub>3</sub>-coated Al nano-size-composite powders using Al, aluminum nitrate and ammonia as the starting materials. Results showed that a uniform thin Al(OH)<sub>3</sub> layer can be formed on the surface of Al particles. After calcined at 1000 °C for 2 h, the thin Al(OH)<sub>3</sub> layer transforms to α-Al<sub>2</sub>O<sub>3</sub> with mean size about 20 nm resulting in well dispersed Al<sub>2</sub>O<sub>3</sub>-Al composite powder [10].

Doan et al. in 2009 studied magnetic chitosan nanoparticles which prepared by the suspension cross-linking technique for use in the application of magnetic carrier technology [11]. Gutkin et al. in 2010 discussed two different modes of delamination in nano-alumina-titania coatings on steel substrates, which are attributed to the conventional fully-melted and the bi-modal fully-melted and partially-melted coating [12].

Olfa et al. in 2012 studied deposition of nano-SiO<sub>2</sub> particles into Zn-Ni alloy coatings in order to improve some surface properties. It had been investigated the effect of loading the plating bath with nanoparticles on composition, morphology, phase structure of deposits, and their subsequent influence on the corrosion process in corrosive solution of 3% NaCl and the thermal stability of deposits at 200°C [13].

The aim of present work is reducing pitting corrosion of pure Al, Al-Si and Al-Zn alloys by nano alumina coating using atomization technique in seawater at room temperature.

## **Experimental Work**

### ***Material and Chemicals***

Specimens of pure aluminium, Al-Si and Al-Zn alloy were polished to mirror finish, degreased with acetone and rinsed with distilled water. These specimens were prepared to achieve nanoalumina coating and corrosion tests in seawater (3.5 wt% NaCl solution). The chemical analysis of pure Al, Al-Si and Al-Zn are shown in table (1) by SpectroMax.

### ***Air Atomizer Coating Technique***

Air atomizer was used as spraying technique which composed of many components: Electrical heater was used to heat the specimen to about 100-150 °C, temperature measurement device as thermocouple was used to measure the specimen temperature, air compressor was used to compress air into the atomizer.

Air atomizer unit, which contains solution container, valve used to control the solution flow and a nozzle with small orifice used to spray the solution (0.5g nano Al<sub>2</sub>O<sub>3</sub> in 100 ml) using the compressed air. The nozzle was directed onto the specimen surface as shown in Figure (1). The nozzle of the air atomizer unit must be placed about (5 cm)

above the specimen which heating of the specimens will help to improve the adhesion between the coating layer and the metal surface.

### ***Electrochemical Cell***

The electrochemical standard cell used in this work was locally fabricated according to the ASTM standard G5-94 with provision for working electrode (Al and its alloys), auxiliary electrode (Pt electrode), and a Luggin capillary for connection with saturated calomel electrode SCE as reference electrode.

### ***Instruments***

Potentiodynamic and cyclic polarization measurements were carried out with WINKING M Lab 200 Potentiostat from Bank-Elektronik. Electrochemical measurements were performed with a potentiostat by SCI electrochemical software at a scan rate  $3 \text{ mV}\cdot\text{sec}^{-1}$ . Polarization experiments were started when the rate at which open circuit potential ( $E_{oc}$ ) changed was less and more 200mV.

The main results obtained were expressed in terms of the corrosion potentials ( $E_{corr}$ ) and corrosion current density ( $i_{corr}$ ) in addition to measure the Tafel slopes by Tafel extrapolation method. From the values of Tafel slopes and corrosion current density, the polarization resistances values can be calculate according to Stern-Geary equation. While experimental parameters for cyclic polarizations were obtained directly from SCI electrochemical software of potentiostat.

### ***AFM measurements***

Microscopic force sensor (cantilever) is used to sense the force between a sharp tip and the sample surface as the sample is scanned to generate an image. Model AA3000 220V from Angstrom Advanced Inc.USA

## **Results and Discussion**

Figs. (2) to (4) show the AFM images of pure Al and its alloys. These figures indicate the coated surface of pure aluminium and its alloys with nanoalumina by atomization technique. Fig. (5) shows the potential – time measurements for uncoated and nanocoated specimens to show the stability of material/environment interface. The coating with nano  $\text{Al}_2\text{O}_3$  shifts the open circuit potential toward active direction, which indicates the film chemistry changes as the potential approaches the steady – state value.

Figs. (6) to (8) show the polarization curves of uncoated and nanocoated specimens of pure Al and its alloys. These curves indicate that the nanocoatings with alumina shift corrosion potential toward active direction and corrosion current density toward lower values especially for cathodic region. The different shapes of polarization curve for experimental samples shows the variation in surface activity with corrosive environment. The uncoated Al and its alloys samples can react with corrosive medium and undergo the corrosion according to the following reactions:



And



However, the decrease in current density is most likely to be attributed to the coating becoming less active in the sense that the pore in the coating are becoming blocked by nano alumina, effectively shielding the substrate and perhaps the coating from the corrosive electrolyte.

Initially, the freshly applied coatings are expected to exhibit a large number of open pores, resulting in the direct exposure of the substrate to the corrosive electrolyte and therefore the subsequent rapid corrosion of the adjacent alumina coating through galvanic interaction. This will result in the localize development of insoluble aluminum corrosion product (aluminum oxides), which will settle in the pores thus blocking the exposure of the substrate to the corrosive electrolyte [14-17]. Ultimately, this process will prevent the flow of ions to the substrate, eliminating the driving force for galvanic corrosion.

Cathodic Tafel slopes were increased, while anodic Tafel slopes were decreased for coated samples compared with uncoated samples. Anodic slopes have values lowers than those of cathodic Tafel slopes. It is inferred that the rate of change of current with change of potential was smaller during anodic polarization than that during cathodic polarization.

The small slope indicates the presence of a film on the surface of the tested material, which is less permeable and can even obstruct the metal dissolution reaction but still permits an electrochemical reaction to occur [18, 19].

The applied nanostructured coating mentioned above on aluminum and its alloys samples showed different degrees of protection capabilities in comparisons with the uncoated specimens in the saline environment used (3.5% NaCl). The best protection efficiency (PE) was achieved for pure Al (80.0%) compared with Al-Si alloy (70.12%) and Al-Zn alloy (57.78%) in spite of the layer have the same particle size of all specimens, this may be due to weak coverage and lower adhesion. Protection efficiency was calculated according to the following formula:

$$PE = \left[ 1 - \frac{i_{coated}}{i_{uncoated}} \right] \times 100$$

Cyclic polarization measurements show that the forward and reverse scan shift toward lower current densities, in addition to the reduction in hysteresis loops for all coated samples compared with uncoated samples as shown in Figure (9).

## Conclusion

Aluminium and its alloys have a passive film in near neutral medium, but this protective film liable to chemically, electrochemically or mechanically breakdown and

then rapid corrosion can occur. In this work, attempt to protect aluminium, Al-Si and Al-Zn alloys by nanoalumina coating was achieved to confirm the protectiveness on the Al and its alloys surface. Nanoalumina coatings were carried out by atomization technique.

Potentiodynamic polarizations show that nanocoatings shift corrosion potentials toward active direction and corrosion current densities toward lower values. Calculations of protection efficiency gave good values especially for pure Al 80% in seawater at room temperature.

## References

- 1- Jaephil Cho, Yong Jeong Kim, and Byungwoo Park, "Novel LiCoO<sub>2</sub> Cathode Material with Al<sub>2</sub>O<sub>3</sub> Coating for a Li Ion Cell", *Chem. Mater.*, Vol. 12 (12), 2000, pp. 3788–3791.
- 2- You Wang, Stephen Jiang, Meidong Wang, Shihe Wang, T.Danny Xiao, Peter R Strutt, "Abrasive wear characteristics of plasma sprayed nanostructured alumina/titania coatings", *Wear*, Vol.237, Issue 2, February 2000, pp. 176–185.
- 3- Jordan E.H., Gell M., Sohn Y.H., Goberman D., Shaw L., Jiang S., Wang M., Xiao T.D., Wang Y., Strutt P., "Fabrication and evaluation of plasma sprayed nanostructured alumina–titania coatings with superior properties", *Materials Science and Engineering:A*, Vol. 301, Issue 1, 15 March 2001, pp. 80–89.
- 4- Jinda Fan, Shaowei Chen, and Yong Gao, "Coating gold nanoparticles with peptide molecules via a peptide elongation approach", *Colloids and Surfaces B: Biointerfaces* Vol. 28, 2003, pp. 199-207.
- 5- Sheng-Chang Wang, Wen-Cheng J Wei, "Kinetics of electroplating process of nano-sized ceramic particle/Ni composite", *Materials Chemistry and Physics*, Vol. 78, Issue 3, 28 February 2003, pp. 574–580.
- 6- Brian G. Prevo and Orlin D. Velev, "Controlled, Rapid Deposition of Structured Coatings from Micro- and Nanoparticle Suspensions", *Langmuir*, Vol.20, 2004, pp. 2099-2107.
- 7- Yulu Wang, Rajesh N. Dave, and Robert Pfeffer, "Polymer coating/encapsulation of nanoparticles using a supercritical anti-solvent process", *J. of Supercritical Fluids*, Vol.28, 2004, pp. 85–99.
- 8- Xinhua Lin, Yi Zeng, Soo Who Lee, Chuanxian Ding, "Characterization of alumina–3 wt.% titania coating prepared by plasma spraying of nanostructured powders", *Journal of the European Ceramic Society*, Vol. 24, Issue 4, April 2004, pp. 627–634.

- 9-** Sheng-Lung Kuo, Yann-Cheng Chen, Ming-Der Ger, Wen-Hwa Hwu, “Nano-particles dispersion effect on Ni/Al<sub>2</sub>O<sub>3</sub> composite coatings”, *Materials Chemistry and Physics*, Vol. 86, Issue 1, 15 July 2004, pp. 5–10.
- 10-** Hong-xia Lu, Jie Hu, Chang-ping Chen, Hong-wei Sun, Xing Hu and De-lin Yang, “Characterization of Al<sub>2</sub>O<sub>3</sub>–Al nano-composite powder prepared by a wet chemical method”, *Ceramics International*, Vol. 31, Issue 3, 2005, pp. 481–485.
- 11-** Doan Thi Kim Dung, Tran Hoang Hai, Le Hong Phuc, Bui Duc Long, Le Khanh Vinh1 and Phan Nha Truc, “Preparation and characterization of magnetic nanoparticles with chitosan coating”, *Journal of Physics: Conference Series* 187, 2009, 012036.
- 12-** Gutkin M. Yu., Mikaelyan K.N. and Ovid’ko I.A., “Enhanced interface toughness in Bi-model nano-alumina-titania coatings”, *Rev.Adv.Mater.Sci.* Vol. 24, 2010, pp.81-85.
- 13-** Olfa Hammami, Leila Dhouibi, Patrice Berc, ElMustafa Rezrazi and Ezzeddine Triki, “Study of Zn-Ni Alloy Coatings Modified by Nano-SiO<sub>2</sub> Particles Incorporation”, Hindawi Publishing Corporation; *International Journal of Corrosion*, Vol., 2012, Article ID 301392, 8 pages.
- 14-** Fischer, K.P., Thomason, W.H., Finnegan, “Electrochemical performance of flame sprayed aluminum coatings of steel in sea water”, *Corrosion* 87, NACE International, No.360, Houston-TX, 1987, USA pp.254,264.
- 15-** Vreijling, M.P.W., “Electrochemical Characterization of Metallic Thermally sprayed Coating”, ISBN 90-9012239-7, 1998 pp.159, 165.
- 16-** Shaw., B.A., Moran, P.J., “Characterization of the corrosion behavior of zinc – aluminum thermal spray coatings”, *Corrosion* 85, NACE International, No.212, Houston-TX, USA, 1985 pp.319, 325.
- 17-** Shaw, B.A., Aylor, D.M., “Barrier Coatings for the Protection of Steel & Aluminum Alloys in The Marine Atmosphere”, Eds. Dean, W.S., Lee, T.S., Degradation of metals in the atmosphere, ASTM, Philadelphia, USA, 1988 pp.206,.
- 18-** Traldi SM, Rossi JL, Costa I., “An electrochemical investigation of the corrosion behavior of Al-Si-Cu hypereutectic alloys in alcoholic environments”, *Revista de Metalurgia Supplementos*, 2003, pp. 86-90.
- 19-** S.M. Traldi, I. Costa, J.L. Rossi, “Corrosion of spray formed Al-Si-Cu alloys in ethanol automobile fuel”, *Key Engineering Materials*, 189-191, 2001, pp.352-357.

**Table (1):** Chemical composition of Al and its alloys.

*Pure Al*

<i>Element</i>	<i>Fe</i>	<i>V</i>	<i>Al</i>
<i>Wt%</i>	0.07	0.13	99.73

*Al-Si alloy*

<i>Element</i>	<i>Si</i>	<i>Fe</i>	<i>Cu</i>	<i>Zn</i>	<i>Mg</i>	<i>Mn</i>	<i>Pb</i>	<i>Cr</i>	<i>Ni</i>	<i>Ti</i>	<i>Al</i>
<i>Wt%</i>	12.74	1.05	1.01	0.49	0.344	0.195	0.1	0.043	0.04	0.03	Bal.

*Al-Zn alloy*

<i>Element</i>	<i>Zn</i>	<i>Mg</i>	<i>Cu</i>	<i>Fe</i>	<i>Si</i>	<i>Mn</i>	<i>Ti</i>	<i>Cr</i>	<i>Al</i>
<i>Wt%</i>	5.1-6.1	2.1-2.9	1.2-2	0.5	0.4	0.3	0.2	0.18-0.28	Bal.

**Table (2):** Corrosion parameters of amalgam in artificial saliva saturated with cigarettes smoking yields at 37°C.

<i>Samples</i>		<i>-E<sub>corr</sub></i> <i>mV</i>	<i>i<sub>corr</sub></i> <i>μA.cm<sup>-2</sup></i>	<i>-b<sub>c</sub></i> <i>mV.dec<sup>-1</sup></i>	<i>b<sub>a</sub></i> <i>mV.dec<sup>-1</sup></i>	<i>PE</i> <i>%</i>
Pure Al	Uncoated	287.7	7.75	117.8	69.4	-
	Coated	311.9	1.55	245.1	16.6	80.00
Al-Si alloy	Uncoated	250.5	4.05	232.4	35.7	-
	Coated	313.8	1.21	426.5	26.0	70.12
Al-Zn alloy	Uncoated	550.6	24.61	265.6	91.6	-
	Coated	684.1	10.39	308.8	44.0	57.78

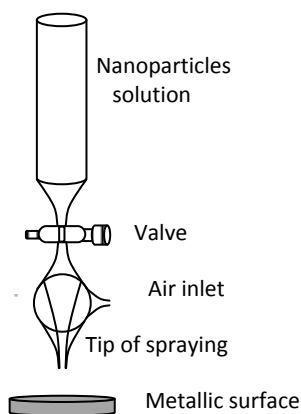


**Fig. (1):** Air atomizer.

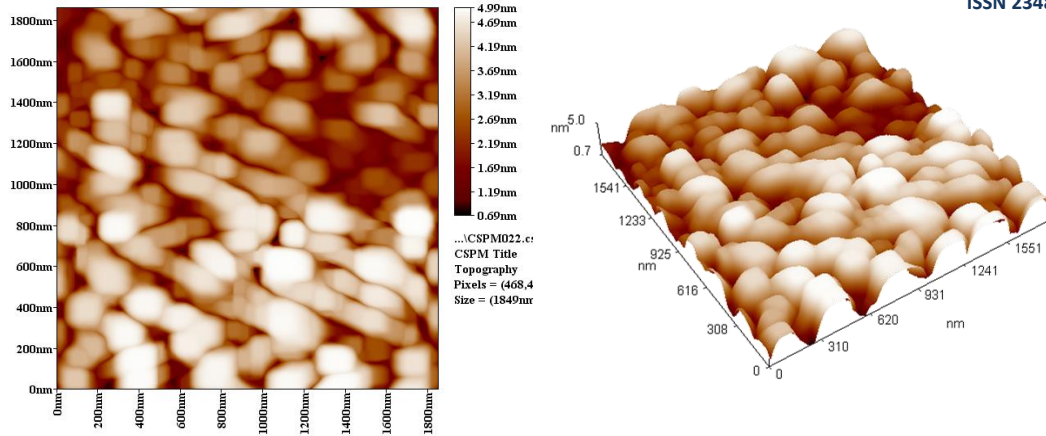


**Fig. (2):** 2D and 3D views of AFM image of  $\text{Al}_2\text{O}_3$  nanoparticles applied on pure Al.

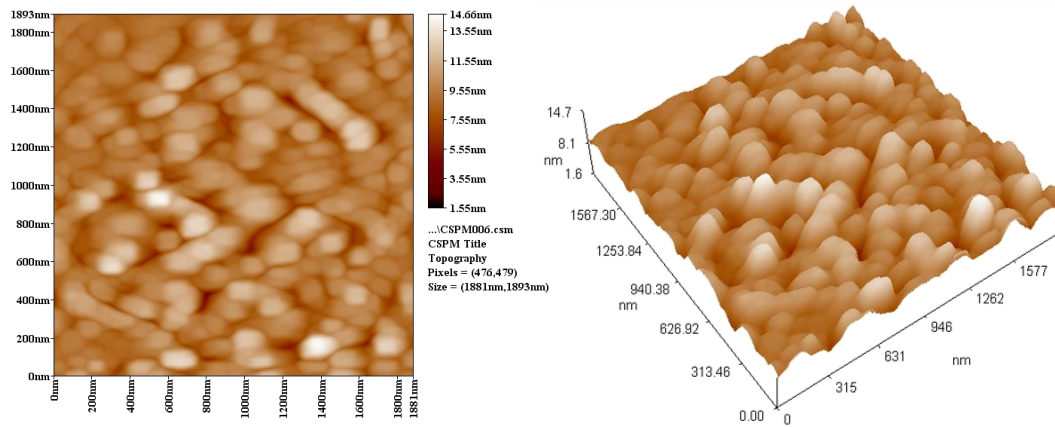


**Fig. (3):** 2D and 3D views of AFM image of  $\text{Al}_2\text{O}_3$  nanoparticles applied on Al-Si alloy.

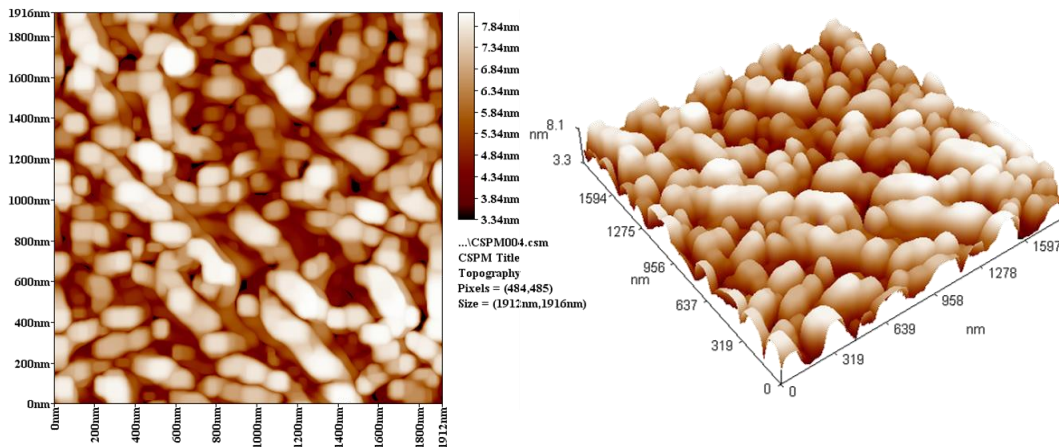


**Fig. (4):** 2D and 3D views of AFM image of  $\text{Al}_2\text{O}_3$  nanoparticles applied on Al-Zn alloy

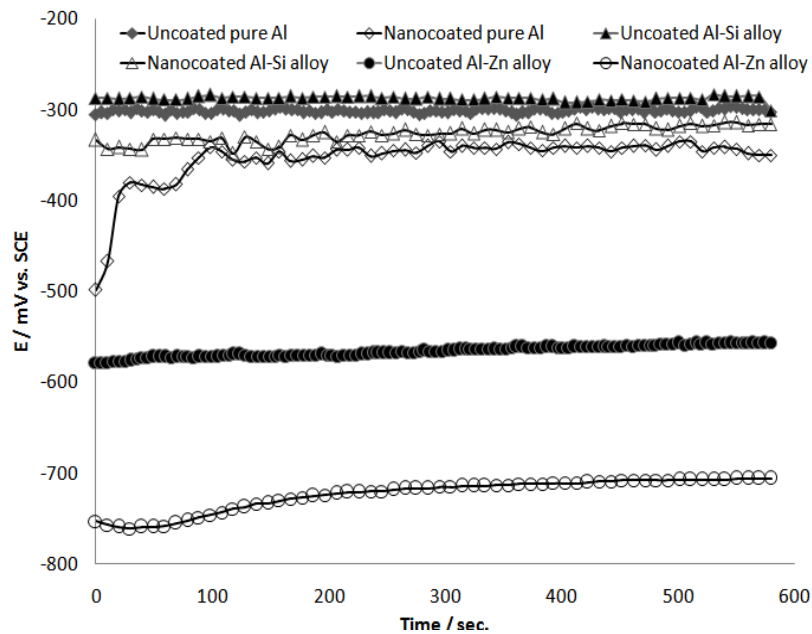


**Fig. (5):** The variation of potential versus time for uncoated and nanocoated pure Al and its alloys in 3.5% M NaCl solution at room temperature.

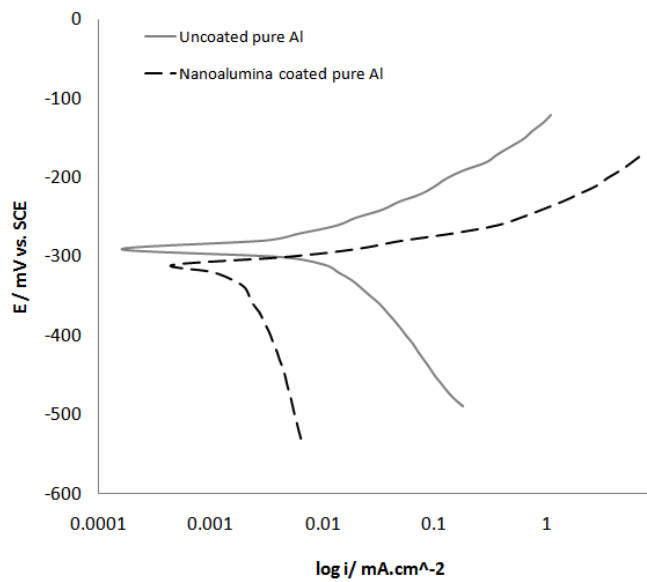


**Fig. (6):** Potentiodynamic polarization for uncoated and nanoaluminum coated pure Al in seawater.

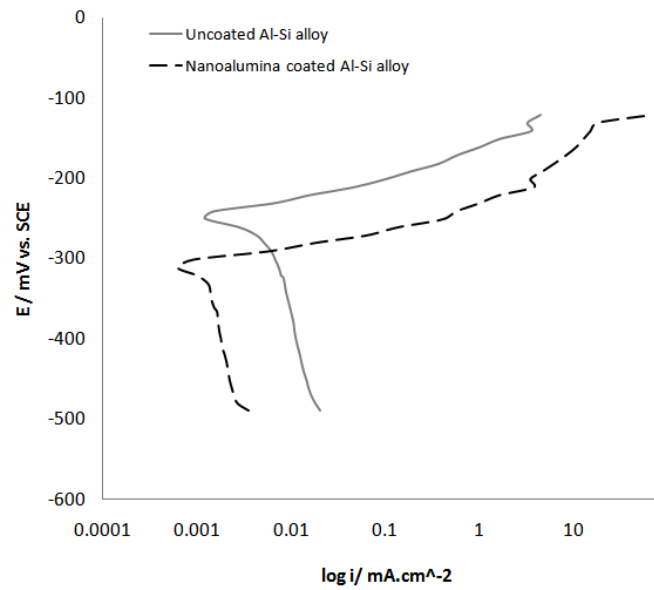


**Fig. (7):** Potentiodynamic polarization for uncoated and nanocoated Al-Si alloy in seawater.

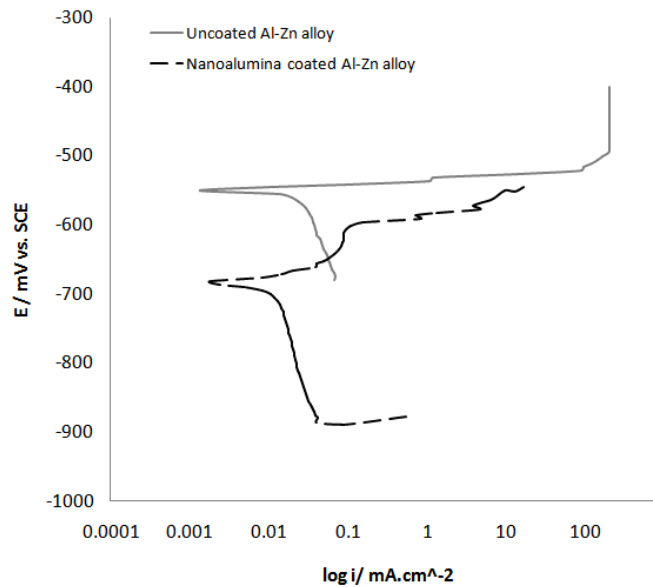


**Fig. (8):** Potentiodynamic polarization for uncoated and nanocoated Al-Zn alloy in seawater.

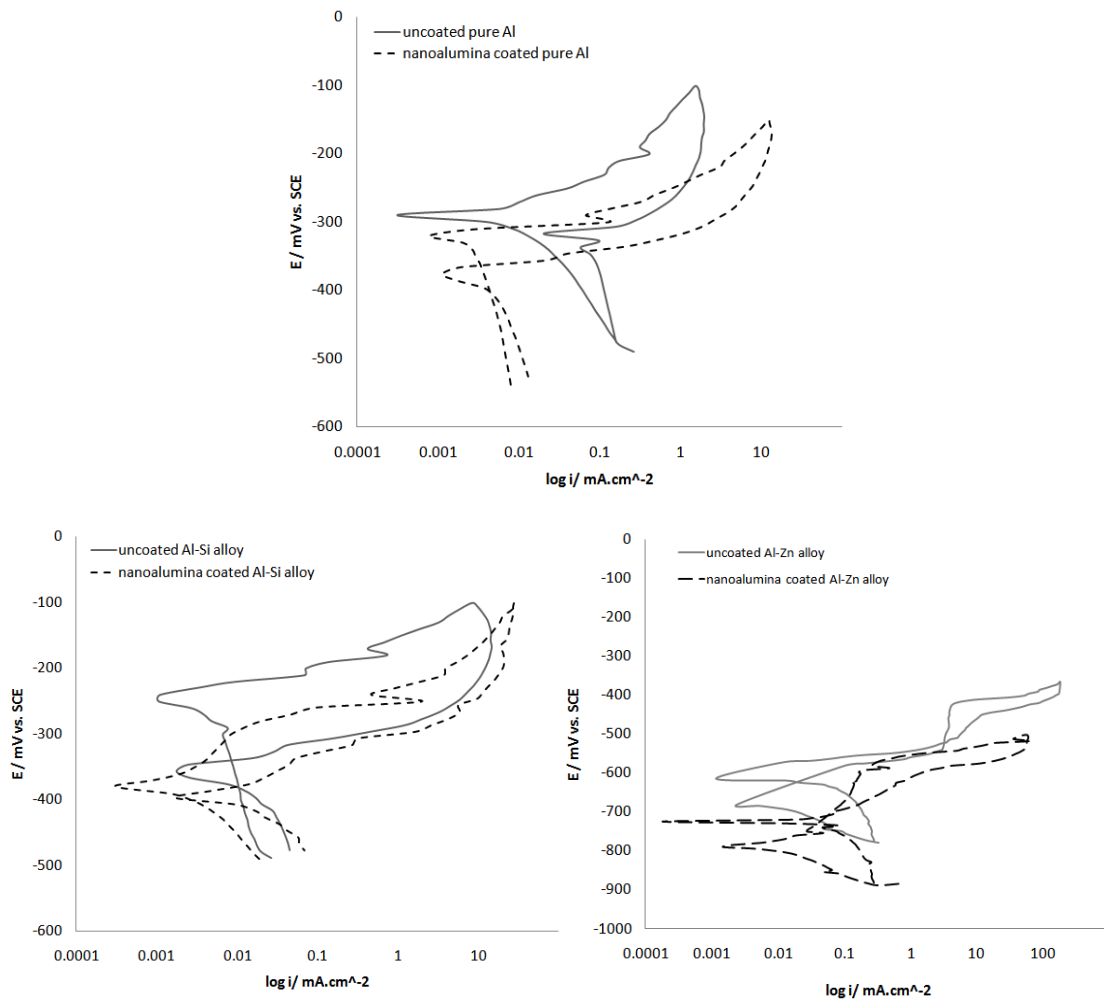


**Fig. (9):** Cyclic polarization for uncoated and nanocoated pure Al and its alloys in seawater.